



## The Use of Remote Sensing Indices for Land Cover Change Detection

### O Uso de Índices de Sensoriamento Remoto para Detecção de Mudanças na Cobertura da Terra

Gustavo Facincani Dourado<sup>1</sup>; Jaíza Santos Motta<sup>1</sup>,  
Antonio Conceição Paranhos Filho<sup>1</sup>; David Findlay Scott<sup>2</sup> & Sandra Garcia Gabas<sup>1</sup>

<sup>1</sup> Universidade Federal de Mato Grosso do Sul, Faculdade de Engenharias, Arquitetura e Urbanismo e Geografia, Cidade Universitária, s/n, 79070-900 Campo Grande, MS, Brasil

<sup>2</sup> The University of British Columbia Okanagan, Department of Earth and Environmental Sciences, I. K. Barber School of Arts and Sciences, 3247, University Way, Kelowna, British Columbia, V1V 1V7, Canada

E-mails: [gustavo.gfd@hotmail.com](mailto:gustavo.gfd@hotmail.com); [ea.jsmotta@gmail.com](mailto:ea.jsmotta@gmail.com);  
[antonio.paranhos@pq.cnpq.br](mailto:antonio.paranhos@pq.cnpq.br); [david.scott@ubc.ca](mailto:david.scott@ubc.ca); [sandra.gabas@gmail.com](mailto:sandra.gabas@gmail.com)

Recebido em: 14/11/2018 Aprovado em: 29/03/2019

DOI: [http://dx.doi.org/10.11137/2019\\_2\\_72\\_85](http://dx.doi.org/10.11137/2019_2_72_85)

#### Abstract

Remote sensing technology has been applied to monitor anthropogenic changes in the landscape that produce impacts on natural resources, such as environmental degradation, changes in the hydrological cycle and in ecosystems structure and functioning. As digital change detection may be a difficult task to perform, this study proposes a simple and logical technique to display land cover changes using Landsat imagery. Open source geoprocessing tools were used to acquire information for mapping changes on the land surface. The Normalized Difference Vegetation Index (NDVI) and Normalized Difference Water Index (NDWI) derived from satellite images of four dates between 1984 and 2016 were used in RGB composites. The method was used to map gains and losses of vegetation cover and liquid water content in a spatiotemporal scale. The results indicate that this change detection method can effectively reflect the variations occurred over the years. Although both indices have similar responses, NDWI may provide opposite information to NDVI in certain areas, such as in wetlands and riparian zones, presenting wetness losses even in places that exhibit gains in vegetation. This method has applicability to other regions for deriving historical changes.

**Keywords:** Landsat; Multi-temporal; NDVI; NDWI; QGIS; Time-series

#### Resumo

A tecnologia de sensoriamento remoto tem sido aplicada para monitorar mudanças antrópicas na paisagem que produzem impactos sobre os recursos naturais, como a degradação ambiental, mudanças no ciclo hidrológico e na estrutura e funcionamento dos ecossistemas. Como a detecção de mudanças de modo digital pode ser uma tarefa difícil de ser realizada, este estudo propõe uma técnica simples e lógica para exibir mudanças na cobertura da terra usando imagens Landsat. Ferramentas de geoprocessamento livres foram usadas para obter informações para mapeamento de mudanças na superfície da terra. O Índice de Vegetação por Diferença Normalizada (NDVI) e o Índice de Diferença Normalizada da Água (NDWI) derivados de imagens de satélite de quatro datas entre 1984 e 2016 foram utilizados em composições RGB. O método foi utilizado para mapear ganhos e perdas de cobertura vegetal e quantidade de água líquida em uma escala espaço-temporal. Os resultados indicam que este método de detecção de mudanças pode efetivamente refletir as variações ocorridas ao longo dos anos. Embora ambos os índices tenham respostas similares, verificou-se que o NDWI pode fornecer informações opostas ao NDVI em certas áreas, como em áreas úmidas e zonas ripárias, apresentando perdas de umidade mesmo em locais que exibem ganhos de vegetação. Esse método tem aplicabilidade para outras regiões para a obtenção de mudanças históricas.

**Palavras-chave:** Landsat; Multitemporal; NDVI; NDWI; QGIS; Séries temporais



## 1 Introduction

Sustainable management of water and land resources is currently a top priority on the agenda of many countries around the world, which demands information on the land cover changes, as they influence the hydrological cycle (Desta *et al.*, 2017). This requires an accurate estimation of present and past dynamics of land use and land cover and its possible consequences. Techniques that combine the use of Remote Sensing (RS) and Geographic Information Systems (GIS) can be easily, quickly, accurately and inexpensively applied for these purposes (Rawat & Kumar, 2015). Therefore, vegetation indices are commonly employed for mapping changes, such as the Normalized Difference Vegetation Index (NDVI) (Rouse *et al.*, 1974; Ceccato *et al.*, 2002a; Lillesand *et al.*, 2008; Sinha *et al.*, 2015; Aburas *et al.*, 2017) and the Normalized Difference Water Index (NDWI) (Gao, 1996; Gu *et al.*, 2008; Campos *et al.*, 2012; Thakkar *et al.*, 2014; Ihuoma & Madramootoo, 2017), which has also been referred to as Normalized Difference Moisture Index (NDMI) or Land Surface Water Index (LSWI) (Beckschäfer, 2017).

Change detection continues to be an area of active research for the development of novel techniques that provide enhanced results (Deilami *et al.*, 2015), as digital change detection may be a difficult task to perform (Coppin *et al.*, 2004). Several procedures can be used to detect land cover changes, such as comparing land cover classifications, multi-temporal classification, image differentiation, vegetation index differentiation, main component analysis and vector variables analysis (Coppin *et al.*, 2004; Mei *et al.*, 2016).

The change detection through a Red-Green-Blue (RGB) color composite has been used to detect changes in forests. Sader & Winne (1992) used three-date NDVI color composites to visualize forest change dynamics, referring to it as RGB-NDVI technique. The RGB-NDVI was also used to provide useful information on monitoring changes in mangrove forest (Pujiono *et al.*, 2013). Hayes & Sader (2001) compared the results of RGB-NDVI, NDVI image differencing and principal component analysis for monitoring tropical forest clearing and veg-

etation regrowth. Their results demonstrate that the RGB-NDVI achieved the highest overall accuracy even with its simple design. Wilson & Sader (2002) used the same technique to detect forest harvest using RGB-NDVI and RGB-NDMI color composites. The RGB-NDMI was also used by Jin & Sader (2005) to detect forest disturbances.

This method is based on the interpretive analysis of three-date RS indices, resulting in images with six colors indicating changes among the study years. Each layer of a RS index is projected simultaneously on the computer screen using the RGB color display channels. This technique is different from the maximum likelihood classification or principal component transformation approaches as these produce images with no logical reference to the date of reflectance change in the raw data channels (Sader & Winne, 1992).

NDVI and NDWI time series may indicate changes in vegetation greenery and liquid water content patterns respectively, in various land cover types, providing information that has not been explored in previous studies. The general land cover types considered for change detection are: burn scar, wildfire, cropland, grassland, native vegetation, commercial forest and wetland.

This study aims to demonstrate and to explain this simple technique that allows the visualization of dynamic changes in land cover, using RS indices in a paired-comparison using RGB-NDVI and RGB-NDWI composites. This approach employs time series of satellite imagery to detect levels of disturbance in vegetation cover and water availability. The objective is to find a suitable RGB combination that provides a better enhancement to visualize changes, to analyze the responses of the indices in two-date RGB color composites for detecting changes over time in both indices and to compare it to the three-date RGB color composite approach.

## 2 Material and Methods

The Landsat scene locations were selected from Path 224 Row 74, based on the Landsat worldwide reference system. For this study, four dates of

satellite imagery were acquired in the dry season (from July to September). The images were selected in the driest months with minimum or no cloud cover, to ensure a better differentiation between the phytophysionomies avoiding incoherent responses caused by phenological changes (Paranhos Filho *et al.*, 2016). All images were recorded by the OLI or TM sensors, acquired without cost from the Earth Explorer page (<http://earthexplorer.usgs.gov>), of the United States Geological Survey (USGS) website. The images used are: Landsat 5 Thematic Mapper (TM sensor), of September 4, 1984, August 20, 1996, August 13, 2005, and the Landsat 8 Operational Land Imager (OLI sensor), of September 28, 2016. The area of overlap of these images is determined as the final study site (Figure 1).

The study site is approximately 3,000,000 hectares, around the municipalities of Ribas do Rio Pardo, Água Clara and Campo Grande. The latter city is the capital of the state of Mato Grosso do Sul (MS) in Brazil. The approximate latitude and longitude are S7840000, S7680000, E150000, and E300000. Most of the area is under cultivated grasslands used for pasture, eucalyptus plantations, and some urban development that includes rivers with dams for urban water supply and hydropower and forest remnants. Soils are derived mainly from sandstones forming a relatively flat terrain. The typical vegetation is the Cerrado, the Brazilian savannah, with a closed to open canopy of deciduous and semi-deciduous forests, closed or open shrubland and natural grasslands (Beuchle *et al.*, 2015). Gallery and riparian forests are extensively found in the Cerrado (Fernandes *et al.*, 2016), many times associated with shrub-herbaceous wetlands (Ratter *et al.*, 1997), grassy wetlands with palms (Meirelles *et al.*, 2002) and palm swamps (Campo Grande, 2008). Often, the springs in these areas are man-made reservoirs for animal watering in the Cerrado (Campo Grande, 2008) and they occur commonly in the study area.

### 2.1 Normalized Difference Vegetation Index

The NDVI, created by Rouse *et al.* (1974), is recognized as the best index used as a numerical indicator of vegetation greenery, since it indicates the amount of chlorophyll and the green cover fraction



Figure 1 Study site in eastern Mato Grosso do Sul (determined as the overlap area of the employed satellite imagery in order to compose time series).

(Ihuoma & Madramootoo, 2017). It uses the red (R) and near-infrared (NIR) bands, therefore NDVI is sensitive to the amount of photosynthetically active vegetation present in the canopy and the amount of biomass (Ponzoni *et al.*, 2015). The NDVI can be calculated using the equation 1:

$$NDVI = (\rho_{NIR} - \rho_R) / (\rho_{NIR} + \rho_R) \quad (1)$$

where: NIR is the reflectance in the near-infrared band (Landsat TM Band 4 or Landsat OLI Band 5); R is the reflectance in the red band (Landsat TM Band 3 or Landsat OLI Band 4). The index varies from -1 to +1, in which the greater the phytomass and density of vegetation, the greater the amount of chlorophyll and the higher the response in this index. High NDVI values represent dense vegetation, such as forests; moderate values, sparse and shrubby vegetation (Thakkar *et al.*, 2014). Likewise, the smaller the chlorophyll content, the lower the response of the index. Therefore, rock, bare soil, barren land show results close to zero (Thakkar *et al.*, 2014). Clouds, water and snow present negative responses (Lillesand *et al.*, 2008).

### 2.2 Normalized Difference Water Index

Gao (1996) proposed the NDWI based on water absorption. This index uses the NIR and short-wave infrared (SWIR) bands, to monitor changes in leaf water content. These bands are related to the quantity of water per unit area in the canopy being able to provide an estimation of water content in terms of equivalent water thickness (Ceccato *et al.*, 2002b). NDWI is sensitive to the water content

of the land surface, responding to surface moisture (wetness), not only to vegetation (Sai & Rao, 2008; Barron *et al.*, 2012; Davies *et al.*, 2016; Mohammadi *et al.*, 2017). The NDWI is derived from the following equation 2:

$$NDWI = (\rho_{NIR} - \rho_{SWIR1}) / (\rho_{NIR} + \rho_{SWIR1}) \quad (2)$$

where:  $\rho_{NIR}$  is the reflectance in the NIR band (Landsat TM Band 4 or Landsat OLI Band 5);  $\rho_{SWIR1}$  is the reflectance in the SWIR band (Landsat TM Band 5 or Landsat OLI Band 6). The index produces values between -1 and +1; values increase with increasing phytomass, indicating that the index is sensitive to the amount of liquid water in vegetation (Campos *et al.*, 2012; Zhang *et al.*, 2016). The SWIR band is highly sensitive to soil water content (Xiao *et al.*, 2002; Dong *et al.*, 2014) and to water itself (Nurdiana & Risdiyanto, 2015) so the NDWI is not free of the effects of background soil reflectance (Ahmed & Akter, 2017). For this reason, its response to each land cover feature is uncertain due to the intrinsic characteristics of water and to the land cover complexity in distinct regions (Campos *et al.*, 2012).

### 2.3 Data Processing

In this study, the open source software QGIS (QGIS Development Team, 2016), constituted of a cross-platform georeferencing system, was used to analyze and process the satellite images for map production. All data were exported to QGIS and re-projected into the WGS84 cartographic system - Universal Transverse Mercator Projection (UTM) 22 S (EPSG: 32722), when necessary. The Landsat data were used because they are georeferenced, orthorectified and atmospherically corrected to surface reflectance by the USGS, with low absolute radiometric calibration uncertainties (Sulla-Menashe *et al.*, 2016). The Landsat 5 images were processed by the Ecosystem Disturbance Adaptive Processing System (LEDAPS) and the Landsat 8 images were processed by the Landsat 8 Surface Reflectance (L8RS) system (Landsat 8 Product Guide) (Zhu *et al.*, 2016). Li *et al.* (2014) compared the response of vegetation indices from Landsat 7 ETM+, which is very similar to the TM sensor, and Landsat 8 OLI imagery over a watershed. The authors found that

the ETM+ sensor and the OLI sensor have a very high consistency of vegetation indices ( $R^2 > 0.99$ ), such as the NDVI and NDWI. Therefore, the data of the TM and OLI sensors, when corrected, correspond to each other properly for their comparison. Topographic effects were taken as negligible as the local relief is mostly flat.

Landsat false-color composites (R - NIR, G - SWIR1, B - Red) for TM and OLI sensors at each date were interpreted after the land cover classifications of Paranhos Filho *et al.* (2006) and Gamarra *et al.* (2016) for the spectral classes found in the Cerrado. In addition, Google Earth was an ancillary tool in the land cover identification process. The NDVI and NDWI for all dates were calculated according to Eq. (1) and (2). The indices were combined to form a time series to provide information over time. After that, the Landsat color composites were compared to the RGB-NDVI and RGB-NDWI.

This analyst driven approach is based on the interpretative analysis of up to three different date images, projected simultaneously on the computer screen using the RGB color display channels (Sader & Winne, 1992). Although the NDVI and NDWI are in grayscale, layers of different sampling years of these indices can be paired with one color band of RGB images creating a “false-color time composite”. Passing the layers of the indices through different combinations in the RGB color gun provide information about land cover changes.

In this way, the indices of different years were combined in pairs to create the RGB color composites (1984-1996, 1996-2005, 2005-2016, 1984-2016). The purpose of mapping different sequences was to evaluate the capacity of identifying changes on different time scales. Afterwards, specific areas were randomly defined for displaying the changes that have been identified in the images.

The layers of different dates are subtracted from each other on a pixel by pixel basis. Depending on the date of the image associated with each display color, the analyst can visualize and assimilate the magnitude and direction of spatiotemporal changes in a landscape in different colors (Hayes & Sader, 2001). Changes are displayed in light to dark colored

tones on a brightness scale in which the greater the change in pixel value between dates, the greater the brightness for gains or losses.

Applying concepts from the additive color synthesis, important changes in land cover between images appear in unique combinations of primary and additive colors, depending on the date of the image associated with the R, G or B display channels (Schroeder *et al.*, 2011). In additive color (CYM) theory, the combination of two primary colors (red, green and blue) will produce a secondary color: C - cyan (green and blue), Y - yellow (red and green) and M - magenta (red and blue). The combination of the three primary colors will produce white, and their absence, black (Pujiono *et al.*, 2013).

The resulting changes in the images were subsequently interpreted to be mostly the result of land use change, through the analysis of Landsat color composites. In this way we detected and identified land cover changes, from which we collected training samples to simultaneously interpret the spectral training signatures that can be used to evaluate and classify changes.

The index value variation from one image to another produces different responses in the resulting composite (Pujiono *et al.*, 2013). This simple and logical technique for change detection is accurate and efficiently allows an easy visual interpretation for time series analysis (Wilson & Sader, 2002). For these reasons, RGB-NDVI and RGB-NDWI composites were selected as the appropriate change detection method to analyze multiple satellite imagery dates in this study. Different band combinations were tested to produce a suitable RGB composite to better distinguish changes.

### 3 Results and Discussion

As different combinations of primary colors with similar brightness produce complementary colors (Pujiono *et al.*, 2013), different arrangements using 2 or 3 of the RGB bands create images with different combinations of primary (RGB) and additive (CYM) colors (Figure 2). The composites using two bands, such as RG produces yellow, green and

red (Figure 2 A); RB produces red, blue and magenta (Figure 2 B); GB produces green, blue and cyan (Figure 2 C). The composites using the three bands produce blue and yellow (Figure 2 D) or red and cyan (Figure 2 E) or green and magenta (Figure 2 F). The order of the bands interferes in the color which gains or losses are shown.

The color composites using two RGB display channels produce tones from dark to light of two primary colors with an additive color transitioning in between (Figure 2 A, B and C). This color gradient between the three colors does not provide a clear visualization for image interpretation. Nevertheless, in the composites resulting from the combination of the three RGB display channels the changes are shown in one primary and one additive color with no color transition in between (Figure 2 D, E and F). The change pixels are clearly distinguished from the grayscale background of the no-change pixels. The green-magenta RGB composite seems to provide a greater enhancement of the changes due to its more pronounced colors. The green-magenta combination was selected as the one that allows a better image visualization and interpretation.

#### 3.1 Comparison of Color Composites

The three-date RGB color composite proposed by Sader & Winne (1992) produces maps with the three primary and the three additive colors varying from white to black. As the additive colors are the product of gradients between the primary colors the resulting maps have a wide range of colors making it difficult to separate and interpret changes. A comparison of RGB-NDWI responses using a three-date composite vs two two-date composites can be seen in Figure 3.

Once the land coverage for each year is known, changes may be classified by type into different spectral clusters (Hayes & Sader, 2001) or by unsupervised classification (Wilson & Sader, 2002; Pujiono *et al.*, 2013), for example. The changes might be classified into different clusters by their intensity in both approaches, what also allows the quantification of the changes. In the three-date series changes may occur twice in the same area, thus

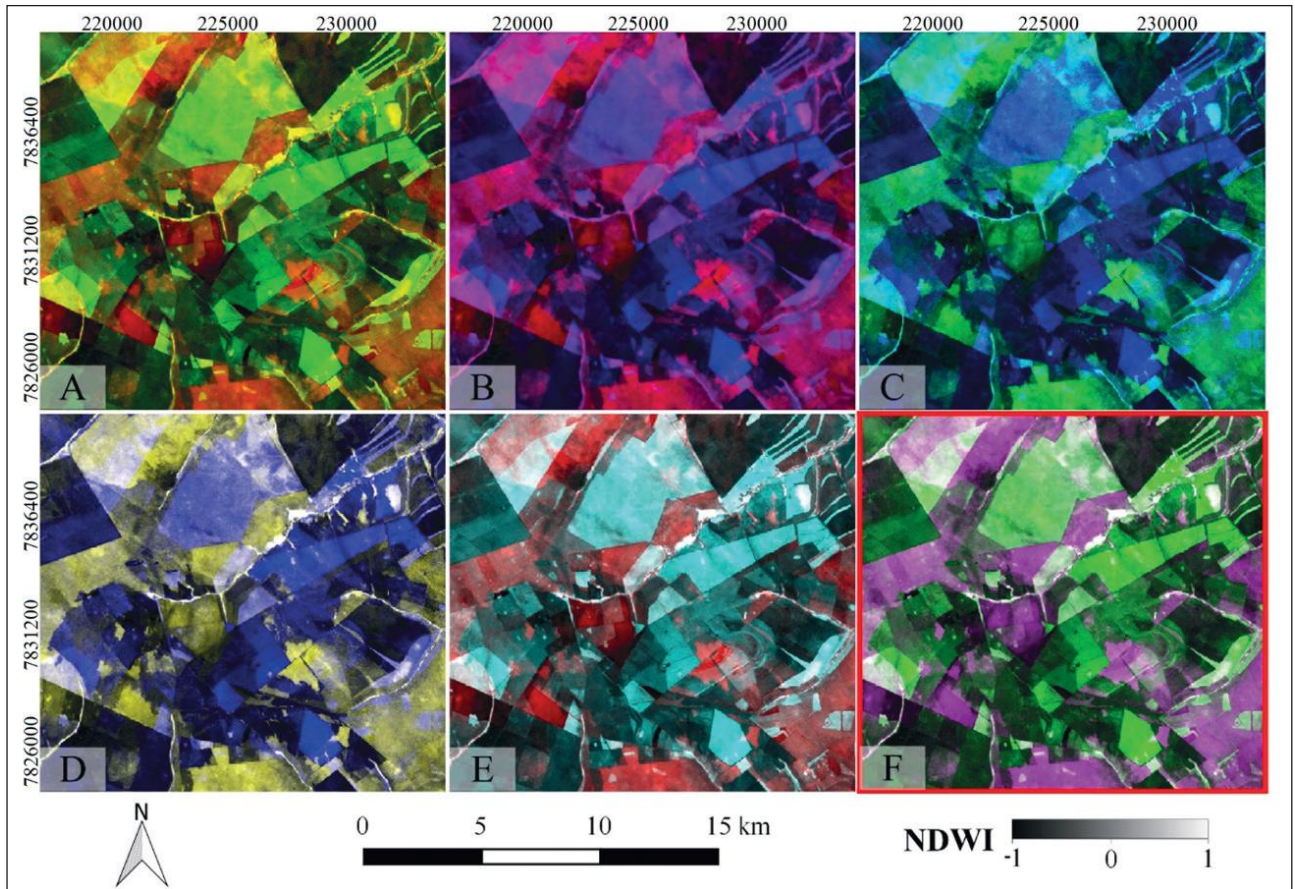


Figure 2 Sample data collection using different RGB-NDWI color composites for change detection. Color composites using NDWI layers in two of the RGB display channels produced: (A) R - 1984, G - 1996, B -, (B) R - 1984, G -, B - 1996, (C) R -, G - 1984, B - 1996; and using the three RGB display channels produced: (D) R - 1984, G - 1984, B - 1996, (E) R - 1984, G - 1996, B - 1996 and the (F) R - 1984, G - 1996, B - 1984 that was selected for this study. The inverse combinations would reverse the color display.

impeding their respective classification in both time periods (Figure 3 D). This does not occur in the two-date series as each time period is evaluated separately (Figure 3 E and F).

Using a one-time period composite to evaluate changes produces an image with half of the information that a two-time period would provide. However, the proposed lower bi-temporal amount of data per composite seems perceptibly simpler and more practical to work with. Bi-temporal time series seemed to yield results that are easily interpreted. The use of two two-date images provides a clearer and quicker understanding of the changes. In the bi-temporal composites, changes can be easily interpreted and classified separately to form a time series of more than two dates.

### 3.2 RGB-NDVI and RGB-NDWI Functioning

The oldest index layer of each of the pairs was assigned to the Red and Blue Bands (producing magenta), and the most recent index layer to the Green Band (producing green) for both indices. As each band represents distinct dates, it is possible to visualize the changes occurring between one date and another. The two layers of each index are subtracted resulting in the RGB image, in which gains appear in green and losses in magenta, in which the greater the change, the brighter the color is. The divergence in colors indicates the relative variation of the reflectance between the two dates, allowing the identification of changes from scrubland to grassland, or from grassland to forest, for example. Training areas were selected to provide understanding of this RGB color composite response in both indices according

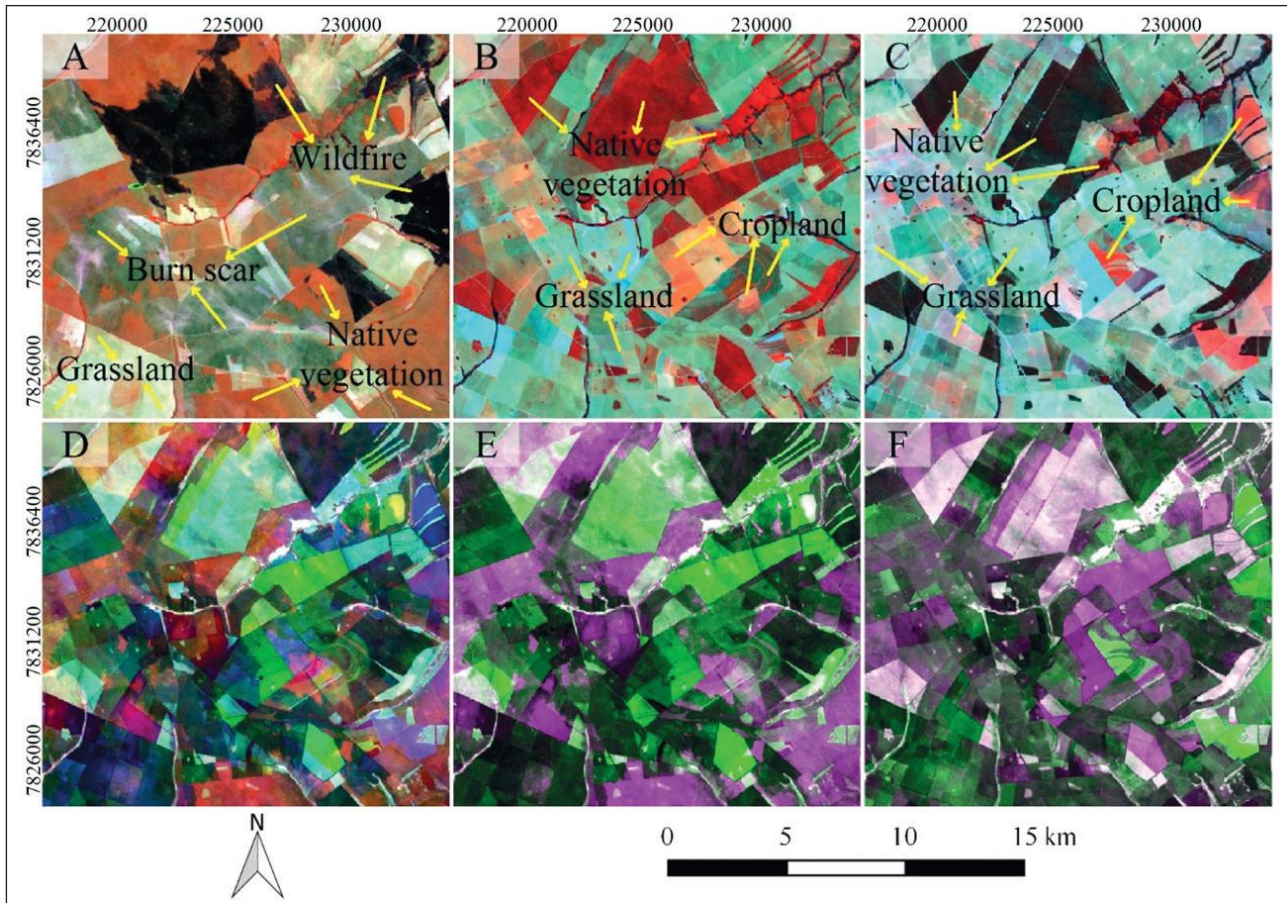


Figure 3 An example of sample data collection using Landsat false-color composite (R - NIR, G - SWIR1, B - Red) of (A) 1984, (B) 1996 and (C) 2005 to identify the land cover features and the RGB-NDWI responses for change detection using a three-date composite (D) R - 1984, G - 1996, B - 2005 vs. two-date composites of (E) R - 1984, G - 1996, B - 1984 and (F) R - 1996, G - 2005, B - 1996. In (D) the changes appear in a wide variety of colors that are difficult to be interpreted, as there are changes occurring in both analyzed periods in the same image, 1984-1996 and 1996-2005. However, dividing these periods into two images allows an easier identification of the changes separately, as seen in (E) and (F), in which the green and magenta colors indicate increase and decrease in NDWI values respectively.

to the land cover changes that can be identified in false-color composites (Figure 4).

The land cover features were identified in the false-color composite. At this point, the land cover changes identified in the training areas were compared to their major response in the RGB-NDVI and NDWI composites (Table 1).

Time series of both indices had great responses in the RGB composite, presenting similar results. NDVI and NDWI have shown a strong linear statistical relationship in vegetation monitoring previously (Karan *et al.*, 2016). Although the temporal NDWI results were found to be similar to those of NDVI but not in all cases, as NDWI responds to vegetation wa-

ter content rather than to chlorophyll as seen in Table 1 (rows 4, 6, 8 and 9). NDVI basically responds to changes in vegetation amount and NDWI not only to vegetation amount but also to moisture/water on the land surface. This explains the low difference in the temporal responses in areas 8 and 9. NDWI presents responses that contrast or even oppose NDVI in certain locations such as in wetlands, as seen in areas 4 and 6 due to the reduced water availability despite the vegetation cover has not decreased or even increased in these areas. Table 2 exemplifies how the green-magenta RGB color composite responds to the relative reflectance variation between the two NDVI or NDWI layers. The analysis of these results can be better understood in Table 3.

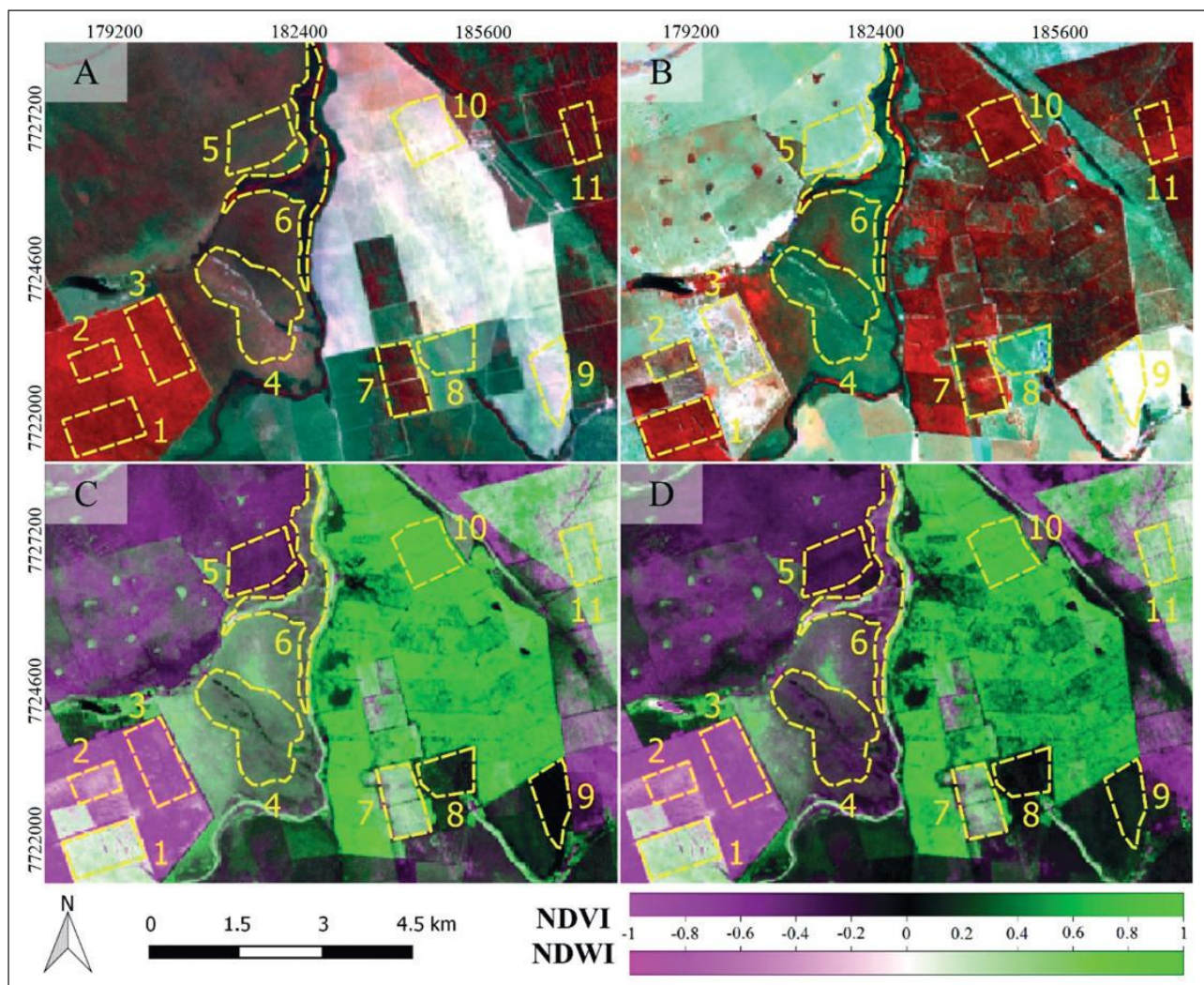


Figure 4 Examples of training areas to visualize changes for each land cover feature by comparison, using Landsat false-color composites (R - NIR, G - SWIR1, B - Red) of (A) 1984 and (B) 2016, and (C) RGB-NDVI and (D) RGB-NDWI composites (R - 1984, G - 1996, B - 1984), indicating changes in vegetation cover and liquid water content, respectively. Gains appear in green and losses in magenta. The yellow lines mark the training areas. The interpretation of these areas is found in Table 1.

Training Areas	Land Cover Feature		Major Response	
	1984	2016	NDVI	NDWI
1	Commercial forest	Commercial forest	White	White
2	Commercial forest	Partially harvested commercial forest	Light magenta	Light magenta
3	Commercial forest	Degraded grassland/shrubland	Bright magenta	Bright magenta
4	Scrub-shrub wetland	Swampy/marshy wetland	Grayish green	Grayish magenta
5	Scrub-shrub vegetation	Dry/tall grassland	Dark magenta	Dark magenta
6	Forested wetland	Swampy/marshy wetland	Grayish	Medium magenta
7	Open forest	Open forest/Dry forest	Light grayish	Light grayish
8	Open grassland	Scrubland	Dark green	Black
9	Dry/low degraded grassland	Dry/low degraded grassland	Black	Dark green
10	Dry/low degraded grassland	Dry forest	Bright green	Bright green
11	Commercial forest	Commercial forest	Light green	Light green

Table 1 Response of each sampled training area in the RGB-NDVI and RGB-NDWI composites (R - 1984, G - 1996, B - 1984) according to land cover changes between 1984 and 2016, according to Figure 4.



The Use of Remote Sensing Indices for Land Cover Change Detection

Gustavo Facincani Dourado; Jaiza Santos Motta, Antonio Conceição Paranhos Filho; David Findlay Scott & Sandra Garcia Gabas






















NDVI or NDWI Layer Pixel Reading					
1984		2016		RGB Composite	
Value	Color	Value	Color	Variation	Color
0.1		0.1		0.0	
0.3		0.3		0.0	
0.8		0.8		0.0	
0.1		0.8		+0.7	
0.1		0.3		+0.2	
0.3		0.1		-0.2	
0.8		0.1		-0.7	

Table 2 Illustrative example of the pixel-by-pixel band subtraction operation of two NDVI or NDWI layers for producing a green-magenta RGB composite (R - 1984, G - 1996, B - 1984).

Color	Indices standard			Interpretation of the NDVI/NDWI
	Red	Green	Blue	
Dark green	Low	Medium	Low	Intermediate increase, in an area with low phytomass/water content
Bright green	Low	High	Low	Significant increase
Light green	Medium	High	Medium	Intermediate increase, in an area with medium phytomass/water content
Dark magenta	Medium	Low	Medium	Intermediate decrease, in an area with low phytomass/water content
Bright magenta	High	Low	High	Significant decrease
Light magenta	High	Medium	High	Intermediate decrease, in an area with high phytomass/water content
White	High	High	High	No change, in an area with high phytomass/water content
Gray	Medium	Medium	Medium	No change, in an area with medium phytomass/water content
Black	Low	Low	Low	No change, in an area with low phytomass/water content

Table 3 Interpretation of the RGB-NDVI and RGB-NDWI (R - 1984, G - 1996, B - 1984), respectively, producing the green-magenta composite, as presented in Table 2.

The RGB-NDVI and RGB-NDWI composites alone cannot be used to categorize land cover changes, as these methods only represent spatiotemporal changes. For example, different vegetation loss standards could occur due to land use change, land degradation, wildfire, thinning, deforestation or harvest. Vegetation gain standards could occur due to agricultural crop yield, native vegetation regrowth, commercial forest growth or reforestation practices.

Both indices, especially NDVI, could identify these changes, but not their causes. Differences in the water levels of waterbodies between images are also confusing responses (Sader & Winne, 1992). Surface waterbodies with expanding or contracting edges could be identified in the NDVI as losses or gains in vegetation, respectively, as water has a lower response than soil and vegetation in this index. On the other hand, NDWI could have the opposite

response, as soil and vegetation are “less wet” than water. Seasonal changes would also present untrue results caused by shifts in NDVI and NDWI due to changes in vegetation greenery and water availability between seasons. To avoid inconsistent responses the best season for data collection is winter for this region, which is the dry period.

Yet, the main utility of this approach is to quickly and easily identify and qualify changes. In this technique, the changes can be visualized and compared, but the results are not fully understandable without knowing the study area. The land cover changes cannot be accurately understood as the method does not enable the analyst to identify the land coverage. Additional sources of remote sensing or in-field data are made necessary in this case. The Landsat color composites with Google Earth as an ancillary tool were enough to discriminate the land cover features and their respective changes in this study.

These data can be easily obtained from any sensor that has the Red, NIR and SWIR bands. The required Landsat data imagery can be obtained at no costs from the USGS, from 1984 to the present. Although timing is difficult due to the presence of clouds and the limited Landsat satellite revisit time. The Landsat images allow the identification of changes in the scale of 1:60,000, that is, objects larger than the pixel size (i.e. 900 m<sup>2</sup>). However, this approach presents ability to process data regardless of the image resolution over large areas using the same rule-base. This method can be applied to other regions once the analyst is familiar with the land cover features of the area, as NDVI and NDWI are spectral indices used to analyze the vegetation covers and water content in a variety of environments.

An agricultural area was selected for displaying examples of changes (Figure 5). Over the years, losses in vegetation cover and liquid water content can be largely observed. Great part of the gains that are seen in the RGB-NDVI and RGB-NDWI composites, mainly in the 1984-1996 composite, are simply due to the fact that several spots had had recently cleared areas for agricultural activities in 1984. Thus, there are several degraded areas,

wildfires, burn scars and bare soil areas especially in 1984, according to the Landsat false-color composites. As these areas were mostly converted into cultivated pastures in the years of comparison, they have mostly green color in both indices in the RGB composites, which indicates gains, but in dark tones, which represents small increases in vegetation cover and wetness (Figure 5).

The RGB-NDWI tends to exhibit darker tones in grasslands (low water content) compared to NDVI (Figure 5 C and D), at least in the analyzed period which is the dry season. Because NDVI responds to chlorophyll in the plant cover, which is not directly and uniformly related to vegetation water amount, it does not have an identical response to the NDWI (Ahmed & Akter 2017). This response shows the great difference in the water content of the canopy of planted pastures relative to other phytophysiological types found in the Cerrado. The change in colors highlight the areas in magenta, that were mostly deforested to become planted pastures. Even though it is a healthy herbaceous vegetation, its water content is much lower than that of the native vegetation. The impacted areas are easily observed using the indices in RGB composites due to the contrast with the gray-scale background.

In Figure 6, the riparian forest was burned and its surroundings were also mostly previously burned in 1984. In 2016, the riparian forest was surrounded by eucalyptus plantations. In this study, a large part of the eucalyptus plantations was found surrounding headwater streams, as in Figure 6 B, which are threatened by human disturbance (Baattrup-Pedersen *et al.*, 2018) mainly those of agricultural activities (Taniguchi *et al.*, 2017). Pronounced wetness losses were found in the burned areas, as highlighted in Figure 6 D, even where there is a vegetation gain, as shown in Figure 6 C. Eucalyptus plantations may also cause a negative impact on the local water resources, as they can reduce groundwater recharge and consequently the discharge in water bodies, altering the local hydrological cycle (Scott & Prinsloo, 2008; Rodríguez-Suárez *et al.*, 2011; Nasta *et al.*, 2017). This fact cannot be disregarded when planning the land use and the technique proposed in this study could be a valuable tool for environmental management.

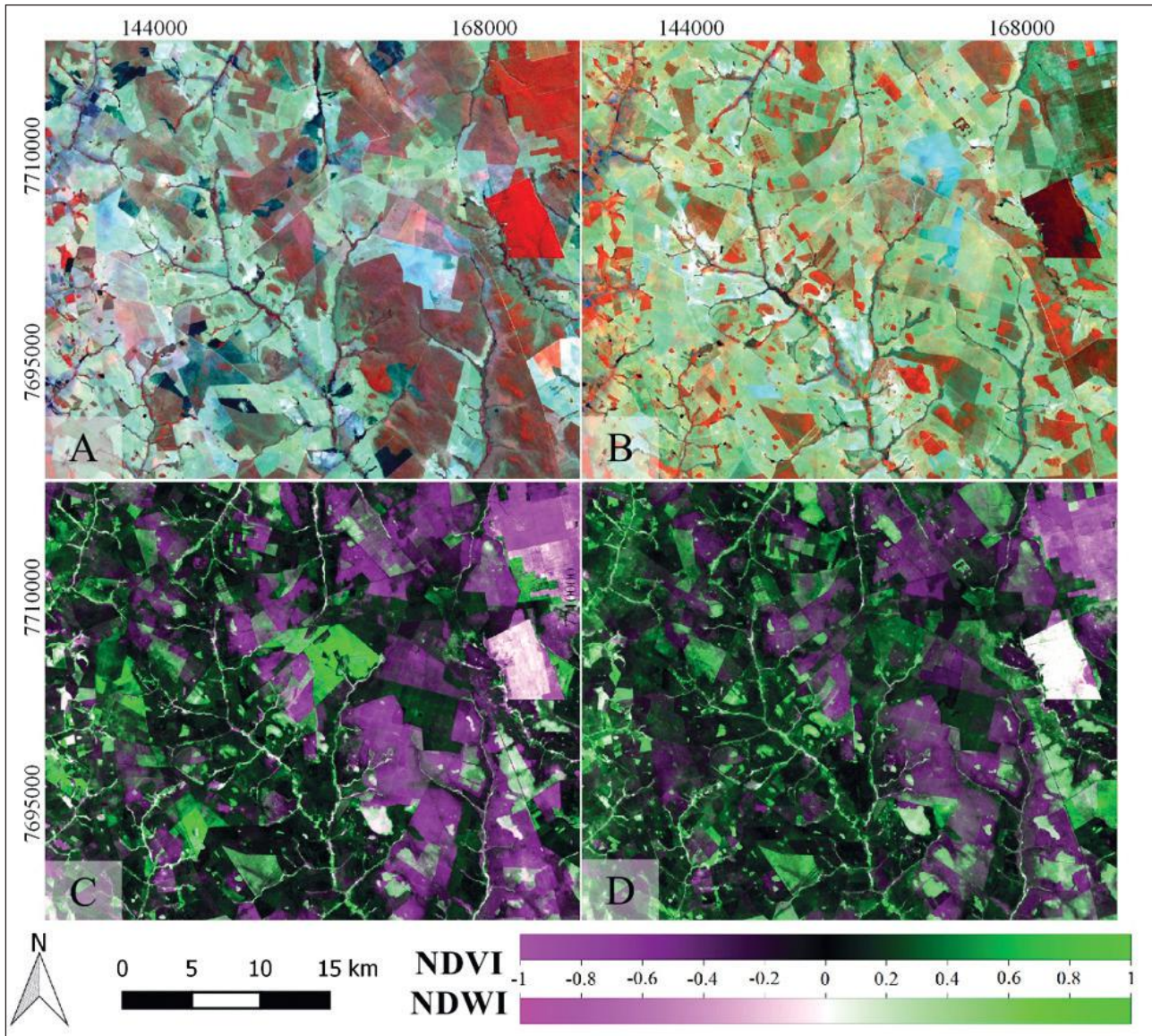


Figure 5 Example of change detection in an agricultural area, using Landsat false-color composites (R - NIR, G - SWIR1, B - Red) of (A) 1984 and (B) 1996, and (C) RGB-NDVI and (D) RGB-NDWI composites (R - 1984, G - 1996, B - 1984), indicating changes in vegetation cover and liquid water content, respectively. Gains appear in green and losses in magenta.

#### 4 Conclusion

The use of remote sensing indices for spatiotemporal analysis provides important information for land surface monitoring, developing improved management strategies and supporting decision-making processes. In this study, the use of two-date RGB-NDVI and RGB-NDWI demonstrated to be able to identify and qualify changes in land cover over time. In order to do that, the

green-magenta RGB composite was chosen as the best option as it promotes a better image visualization and interpretation.

The RGB-NDVI and RGB-NDWI composites alone cannot be used to categorize land cover changes, as this method represents spatiotemporal changes. However, additional remote sensing information were enough to identify and categorize the land cover features in this study. The approach reported here

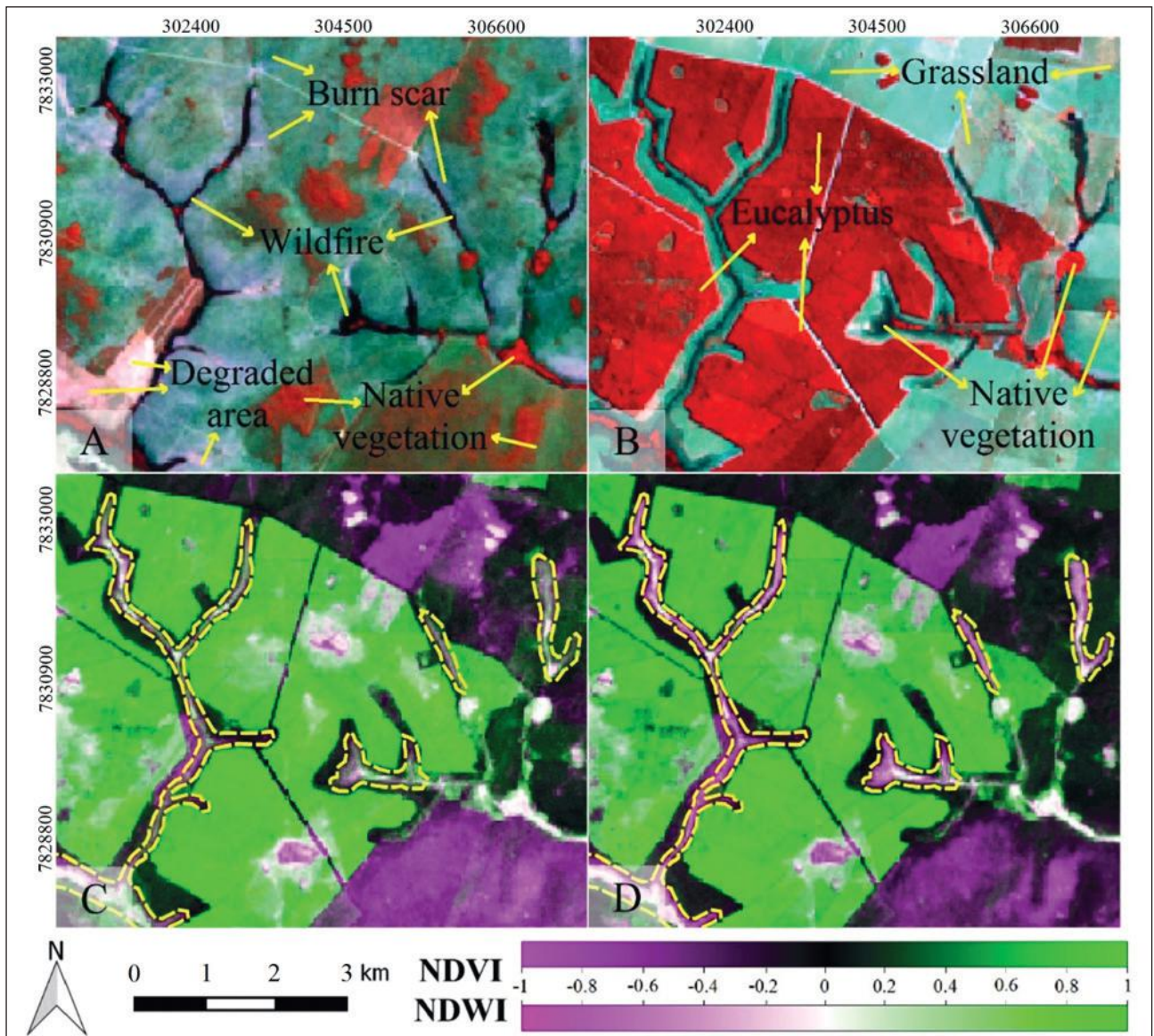


Figure 6 Headwater streams identified using Landsat false color composites (R - NIR, G - SWIR1, B - Red) of (A) 1984 and (B) 2016, and (C) RGB-NDVI and (D) RGB-NDWI composites (R - 1984, G - 1996, B - 1984), indicating changes in vegetation cover and liquid water content, respectively. Gains appear in green and losses in magenta. The yellow lines mark the areas in which the responses of the indices are distinguishably different.

was found to be a better alternative than the three-date composite. It is a simple, easy and quick means to visualize and quantify the changes in vegetation and liquid water content patterns, that can be easily applied to other regions on different scales once the land surface is known.

RGB-NDVI and RGB-NDWI have similar visual responses most of the time. In certain areas they may show different responses in ways that proved to be useful in this study. The differences between the indices might indicate the impact of human-induced land use change on the hydrolog-

ical cycle causing the modification of riparian and wetland ecosystems. NDVI and NDWI are proven spectral indices to do trend analysis of the vegetation covers and water content in a temporal resolution and in a variety of environments.

## 5 Acknowledgments

The Brazilian Coordination for the Improvement of Higher Level Education Personnel (CAPES) through the Graduate Program in Environmen-

tal Technology (PGTA/UFMS) and the Emerging Leaders in the Americas Program (ELAP), funded by the Department of Foreign Affairs, Trade and Development (DFATD) are gratefully acknowledged for granting a master's scholarship and an exchange program award, respectively, to Gustavo Facincani Dourado. The Support Foundation for the Development of Education, Science and Technology in the State of Mato Grosso do Sul (FUNDECT) and the Brazilian National Council for Scientific and Technological Development (CNPq) are also acknowledged for granting a master's scholarship to Jaiza Santos Motta (Process 71/700.174/2017) and a research grant to Antonio Conceição Paranhos Filho (Process 304122/2015-7) respectively.

## 6 References

- Aburas, M.M.; Abdullah, S.H.; Ramli, M.F. & Ash'aari, Z. 2015. Measuring land cover change in Seremban, Malaysia using NDVI index. *Procedia Environmental Sciences*, 30:238-243.
- Ahmed, K.R. & Akter, S. 2017. Analysis of landcover change in southwest Bengal delta due to floods by NDVI, NDWI and K-means cluster with Landsat multi-spectral surface reflectance satellite data. *Remote Sensing Applications: Society and Environment*, 8:168-181.
- Baatrup-Pedersen, A.; Larsen, S.E.; Andersen, D.K.; Jepsen, N.; Nielsen, J. & Rasmussen, J.J. 2018. Headwater streams in the EU Water Framework Directive: Evidence-based decision support to select streams for river basin management plans. *Science of the Total Environment*, 613:1048-1054.
- Barron, O.V.; Emelyanova, I.; Van Niel, T.G.; Pollock, D. & Hodgson, G. 2014. Mapping groundwater-dependent ecosystems using remote sensing measures of vegetation and moisture dynamics. *Hydrological Processes*, 28(2):372-385.
- Beckschäfer, P. 2017. Obtaining rubber plantation age information from very dense Landsat TM & ETM+ time series data and pixel-based image compositing. *Remote Sensing of Environment*, 196:89-100.
- Beuchle, R.; Grecchi, R.C.; Shimabukuro, Y.E.; Seliger, R.; Eva, H.D.; Sano, E. & Achard, F. 2015. Land cover changes in the Brazilian Cerrado and Caatinga biomes from 1990 to 2010 based on a systematic remote sensing sampling approach. *Applied Geography*, 58:116-127.
- Campo Grande, P.M. 2008. Plano de Manejo da Área de Proteção Ambiental dos Mananciais do Córrego Guariroba-APA do Guariroba. Campo Grande, MS: PMCG.
- Campos, J.C.; Sillero, N. & Brito, J.C. 2012. Normalized difference water indices have dissimilar performances in detecting seasonal and permanent water in the Sahara-Sahel transition zone. *Journal of Hydrology*, 464:438-446.
- Ceccato, P.; Flasse, S. & Gregoire, J. 2002a. Designing a spectral index to estimate vegetation water content from remote sensing data: Part 2. Validation and applications. *Remote Sensing of Environment*, 82(2):198-207.
- Ceccato, P.; Gobron, N.; Flasse, S.; Pinty, B. & Tarantola, S. 2002b. Designing a spectral index to estimate vegetation water content from remote sensing data: Part 1. Theoretical approach. *Remote Sensing of Environment*, 82:188-197.
- Coppin, P.; Jonckheere, I.; Nackaerts, K.; Muys, B. & Lambin, E. 2004. Digital change detection methods in natural ecosystem monitoring: A review. *International Journal of Remote Sensing*, 25(9):1565-1596.
- Davies, T.; Everard, M. & Horswell, M. 2016. Community-based groundwater and ecosystem restoration in semi-arid north Rajasthan (3): Evidence from remote sensing. *Ecosystem Services*, 21:20-30.
- Deilami, B.R.; Ahmad, B.B.; Saffar, M.R.A. & Umar, H.Z. 2015. Review of change detection techniques from remotely sensed images. *Research Journal of Applied Sciences, Engineering and Technology*, 10(2):221-229.
- Desti, H.; Lemma, B. & Gebremariam, E. 2017. Identifying sustainability challenges on land and water uses: The case of Lake Ziway watershed, Ethiopia. *Applied Geography*, 88:130-143.
- Dong, Z.; Wang, Z.; Liu, D.; Song, K.; Li, L.; Jia, M. & Ding, Z. 2014. Mapping wetland areas using Landsat-derived NDVI and LSWI: A case study of West Songnen plain, Northeast China. *Journal of the Indian Society of Remote Sensing*, 42(3):569-576.
- Fernandes, G.W.; Coelho, M.S.; Machado, R.B.; Ferreira, M.E.; Aguiar, L.M.S.; Dirzo, R.; Scariot, A. & Lopes, C.R. 2016. Afforestation of savannas: an impending ecological disaster. *Natureza & Conservação*, 14(2):146-151.
- Gamarra, R.M.; Ferreira, T.S.; Roche, K.F.; Matos Filho, H.J.S.; Catalani, T.G.T.; Pagotto, T.C.S. & Paranhos Filho, A.C. 2016. Análise das Mudanças da Cobertura do Solo de uma Área de Cerrado (Savana Tropical) no Centro-Oeste do Brasil. *Anuário do Instituto de Geociências*, 39(1):76-90.
- Gao B. 1996. NDWI - A normalized difference water index for remote sensing of vegetation liquid water from space. *Remote Sensing of Environment*, 58(3):257-266.
- Gómez, C.; White, J.C.; Wulder, M.A. & Alejandro, P. 2015. Integrated object-based spatiotemporal characterization of forest change from an annual time series of Landsat image composites. *Canadian Journal of Remote Sensing*, 41(4):271-292.
- Gu, Y.; Hunt, E.; Wardlow, B.; Basara, J.B.; Brown, J.F. & Verdin, J.P. 2008. Evaluation of MODIS NDVI and NDWI for vegetation drought monitoring using Oklahoma Mesonet soil moisture data. *Geophysical Research Letters*, 35(22):1-5.
- Hayes, D.J. & Sader, S.A. 2001. Comparison of change-detection techniques for monitoring tropical forest clearing and vegetation regrowth in a time series. *Photogrammetric Engineering and Remote Sensing*, 67(9):1067-1075.
- Ihuoma, S.O. & Madramootoo, C.A. 2017. Recent advances in crop water stress detection. *Computers and Electronics in Agriculture*, 141:267-275.
- Jin, S. & Sader, S.A. 2005. Comparison of time series tasseled cap wetness and the normalized difference moisture index in detecting forest disturbances. *Remote Sensing of Environment*, 94(3): 364-372.
- Karan, S.K.; Samadder, S.R. & Maiti, S.K. 2016. Assessment of the capability of remote sensing and GIS techniques for monitoring reclamation success in coal mine degraded lands. *Journal of Environmental Management*, 182:272-283.
- Li, P.; Jiang, L.; & Feng, Z. 2014. Cross-comparison of vegetation indices derived from Landsat-7 enhanced thematic mapper

- plus (ETM+) and Landsat-8 operational land imager (OLI) sensors. *Remote Sensing*, 6(1), 310-329.
- Lillesand, T.M.; Kiefer, R.W. & Chipman, J.W. 2004. Remote Sensing and Image Interpretation, fifth ed. John Wiley & Sons Inc., New York.
- Mei, A.; Manzo, C.; Fontinovo, G.; Bassani, C.; Allegrini, A. & Petracchini, F. 2016. Assessment of land cover changes in Lampedusa Island (Italy) using Landsat TM and OLI data. *Journal of African Earth Sciences*, 122:15-24.
- Meirelles, M.L.; Oliveira, R.C.; Vivaldi, L.J.; Santo, A.D. & Correia, J.R. 2002. Espécies de estrato herbáceo e profundidade do lençol freático em áreas úmidas do Cerrado. *Embrapa Cerrados*.
- Mohammadi, A.; Costelloe, J.F. & Ryu, D. 2017. Application of time series of remotely sensed normalized difference water, vegetation and moisture indices in characterizing flood dynamics of large-scale arid zone floodplains. *Remote Sensing of Environment*, 190:70-82.
- Nasta, P.; Palladino, M.; Ursino, N.; Saracino, A.; Sommella, A. & Romano, N. 2017. Assessing long-term impact of land-use change on hydrological ecosystem functions in a Mediterranean upland agro-forestry catchment. *Science of the Total Environment*, 605:1070-1082.
- Nurdiana, A. & Risdiyanto, I. 2015. Indicator determination of forest and land fires vulnerability using Landsat-5 TM data (case study: Jambi Province). *Procedia Environmental Sciences*, 24: 141-151.
- Paranhos Filho, A.C.; Gamarra, R.M.; Pagotto, T.C.; Ferreira, T.S.; Torres, T.G. & Matos Filhos, H.J.S. 2006. Sensoriamento Remoto do Complexo Aporé-Sucuriú. Biodiversidade do Complexo Aporé-Sucuriú: subsídios à conservação e manejo do bioma Cerrado. Editora UFMS. Campo Grande.
- Paranhos Filho, A.C.; Mioto, C.L.; Marcato Junior, J. & Catalani, T.G.T. 2016. Geotecnologias em aplicações ambientais. Editora UFMS. Campo Grande.
- Ponzoni, F.J.; Shimabukuro, Y.E. & Kuplich, T.M. 2015. Sensoriamento remoto da vegetação. Second ed. Oficina de Textos., São Paulo.
- Pujiono, E.; Kwak, D.; Lee, W.; Sulistyanto; Kim, S.; Lee, J.Y.; Lee, S.; Park, T. & Kim, M. 2013. RGB-NDVI color composites for monitoring the change in mangrove area at the Maubesi Nature Reserve, Indonesia. *Forest Science and Technology*, 9(4):171-179.
- QGIS Development Team. 2017. QGIS Geographic Information System. Open Source Geospatial Foundation Project. Available in: <<http://www.qgis.org/>>. Accessed: April 10, 2017
- Ratter, J.A.; Ribeiro, J.F. & Bridgewater, S. 1997. The Brazilian cerrado vegetation and threats to its biodiversity. *Annals of Botany*, 80(3):223-230.
- Rawat, J.S. & Kumar, M. 2015. Monitoring land use/cover change using remote sensing and GIS techniques: A case study of Hawalbagh block, district Almora, Uttarakhand, India. *The Egyptian Journal of Remote Sensing and Space Science*, 18(1):77-84.
- Rodríguez-Suárez, J.A.; Soto, B.; Perez, R. & Diaz-Fierros, F. 2011. Influence of Eucalyptus globulus plantation growth on water table levels and low flows in a small catchment. *Journal of Hydrology*, 396(3-4):321-326.
- Rouse, J.; Hass, R.; Schell, J.A. & Deering, D.W. 1973. Monitoring the Vernal Advancement and Retrogradation (Greenwave Effect) of Natural Vegetation. College Station, Remote Sensing Center, Texas A&M University, 362 p.
- Sader, S.A. & Winne, J.C. 1992. RGB-NDVI colour composites for visualizing forest change dynamics. *International Journal of Remote Sensing*, 13(16):3055-3067.
- Schroeder, T.A.; Wulder, M.A.; Healey, S.P. & Moisen, G.G. 2011. Mapping wildfire and clearcut harvest disturbances in boreal forests with Landsat time series data. *Remote Sensing of Environment*, 115(6):1421-1433.
- Scott, D.F. & Prinsloo, F.W. 2008. Longer-term effects of pine and eucalypt plantations on streamflow. *Water Resources Research*, 44(7):1-8.
- Sinha, S.; Sharma, L.K. & Nathawat, M.S. 2015. Improved land-use/land-cover classification of semi-arid deciduous forest landscape using thermal remote sensing. *The Egyptian Journal of Remote Sensing and Space Science*, 18(2):217-233.
- Sulla-Menashe, D.; Friedl, M.A. & Woodcock, C.E. 2016. Sources of bias and variability in long-term Landsat time series over Canadian boreal forests. *Remote Sensing of Environment*, 177:206-219.
- Taniwaki, R.H.; Cassiano, C.C.; Filoso, S.; Barros Ferraz, S.F.; Camargo, P.B. & Martinelli, L.A. 2017. Impacts of converting low-intensity pastureland to high-intensity bioenergy cropland on the water quality of tropical streams in Brazil. *Science of the Total Environment*, 584:339-347.
- Thakkar, A.K.; Desai, V.; Patel, A. & Potdar, M. 2014. Land use/land cover classification of remote sensing data and their derived products in a heterogeneous landscape of a Khan-Kali watershed, Gujarat. *Asian Journal of Geoinformatics*, 14(4):1-12.
- Wilson, E.H. & Sader, S.A. 2002. Detection of forest harvest type using multiple dates of Landsat TM imagery. *Remote Sensing of Environment*, 80(3):385-396.
- Xiao, X.; Boles, S.; Froking, S.; Salas, W.; Moore III, B. & Li, C. 2002. Observation of flooding and rice transplanting of paddy rice fields at the site to landscape scales in China using VEGETATION sensor data. *International Journal of Remote Sensing*, 23(15):3009-3022.
- Zhang, K.; Thapa, B.; Ross, M. & Gann, D. 2016. Remote sensing of seasonal changes and disturbances in mangrove forest: a case study from South Florida. *Ecosphere*, 7(6):1-12.
- Zhu, W.; Fu, Y.; Woodcock, C.E.; Olofsson, P.; Vogelmann, J.E.; Holden, C.; Wang, M.; Dai, S. & Yu, Y. 2014. An assessment of remote sensing algorithms for colored dissolved organic matter in complex freshwater environments. *Remote Sensing of Environment*, 140: 766-778.